Crossover from antiferromagnetic to ferromagnetic ordering in TmCuSi by neutron diffraction

ARTICLE *in* JOURNAL OF MAGNETISM AND MAGNETIC MATERIALS · JUNE 2002

Impact Factor: 1.97 · DOI: 10.1016/S0304-8853(02)00180-4

ELSEVIER

Journal of Magnetism and Magnetic Materials 247 (2002) 207–214

journal of magnetism and magnetic materials

www.elsevier.com/locate/jmmm

Crossover from antiferromagnetic to ferromagnetic ordering in TmCuSi by neutron diffraction

P. Schobinger-Papamantellos[a,*], C. Ritter[b], K.H.J. Buschow[c], N.P. Duong[c]

[a] *Laboratorium für Kristallographie, ETHZ CH-8092 Zürich, Switzerland*
[b] *Institut Laue-Langevin, 156X, 38042 Grenoble Cédex, France*
[c] *Van der Waals-Zeeman Institute, University of Amsterdam Valckenierstr. 65, 1018 XE Amsterdam, Netherlands*

Received 11 January 2002

Abstract

The previously reported ferromagnetic TmCuSi ($P6_3/mmc$) compound ($T_N = 9\,K$) has been reinvestigated by neutron powder diffraction and was found to order antiferromagnetically at $T_N = 6.5(1)\,K$ with a sine wave modulated structure $\mathbf{q}_1 = (q_x, 0, 0)$ with the Tm moments deviating from the *c*-axis. This phase is restricted to a narrow high-temperature range 5.1–6.5 K where the wave vector decreases linearly by only 9% (from $q_x = 0.078$ to 0.071, on cooling). However, below $T_C = 5.8\,K$ by a first-order transition the wave vector jumps to the value $\mathbf{q}_2 = 0$ giving rise to ferromagnetic ordering which dominates in the low-temperature range. The two phases coexist in temperature-dependent portions in the intermediate range $5.4 \pm 0.4\,K$. This transition is associated with a reorientation of the Tm moments towards the *c*-axis below T_C. The saturation ordered moment value of $6.2(1)\,\mu_B$/atom at 1.5 K is reduced relatively to the Tm^{3+} free ion moment value of $g\mu_B J = 7\,\mu_B$. © 2002 Elsevier Science B.V. All rights reserved.

Keywords: Rare earths; Neutron diffraction; Magnetic ordering

1. Introduction

The crystal structure and magnetic properties of the RCuSi (R = rare earth) compounds have been reported in several investigations [1–9]. These compounds crystallise with two types of structure depending on the annealing temperature. The high-temperature (HT) phase adopts the AlB_2-type [2] (P6/mmm, R at 1*a*: (0 0 0) Cu/Si statistically occupy the 2*d* site: (1/3, 2/3, 1/2)). The low-temperature (LT) phase is of the Ni_2In type [3,4] (space group $P6_3/mmc$ Ni at 2*a*: (0 0 0) and 2*c*: (1/3, 2/3, 1/4) and In in 2*d*: (1/3, 2/3, 3/4). The Cu and Si atoms are located at the 2*c* and 2*d* sites, respectively (see Fig. 1). According to Ref. [5] the AlB_2-type RCuSi (R = Pr, Gd, Tb) compounds order ferromagnetically (F). Kido et al. [6] suggest on the basis of magnetic susceptibility measurements that the compounds with R = Ce, Nd order antiferromagnetically while those with R = Gd, Ho order ferromagnetically. Neutron diffraction experiments performed on the RCuSi (R = Tb, Dy, Ho, Er) compounds with the Ni_2In type of structure showed that the compounds with R = Dy, Ho do not order down to 4.2 K, whereas

*Corresponding author. Tel.: +41-1-632-37-73; fax: +41-1-632-11-33.
E-mail address: schobinger@kristall.erdw.ethz.ch (P. Schobinger-Papamantellos).

0304-8853/02/$ - see front matter
PII: S0304-8853(02)00180-4

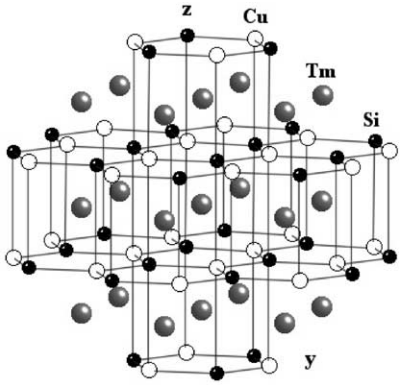

Fig. 1. Schematic representation of the crystal structure of TmCuSi.

the TbCuSi [7] and ErCuSi [8] compounds order antiferromagnetically below $T_N = 16$ and 6.8 K with transversal amplitude modulated structures associated with the wave vectors $\mathbf{q} = (1/20, 0, 1/2)$ and $(1/12, 0, 0)$, respectively. The Tb^{3+} moments are in the basal plane and make an angle of 79° with the *a*-axis while the Er^{3+} moments point to the *c*-axis. Surprisingly, the TmCuSi compound with the same Ni_2In-type of structure was reported to order ferromagnetically at a higher temperature ($T_C = 9$ K) than that of ErCuSi and with the moments parallel to the *c*-axis [9]. The present paper revises the results on the magnetic ordering of TmCuSi reported in Ref. [9] where this phase was present as the minority phase in a two-phase sample.

2. Experimental

A sample of TmCuSi was prepared by arc melting of the elements under purified argon. Subsequently the sample was vacuum annealed at 700°C for 3 weeks. The sample was characterized by X-ray diffraction and found to adopt the Ni_2In structure and to contain a small amount of an unknown impurity phase with one non-overlapping reflection. The magnetic measurements were carried out in a Quantum Design SQUID magnetometer.

Neutron diffraction data were collected with the double axis multicounter-diffractometers D1B and

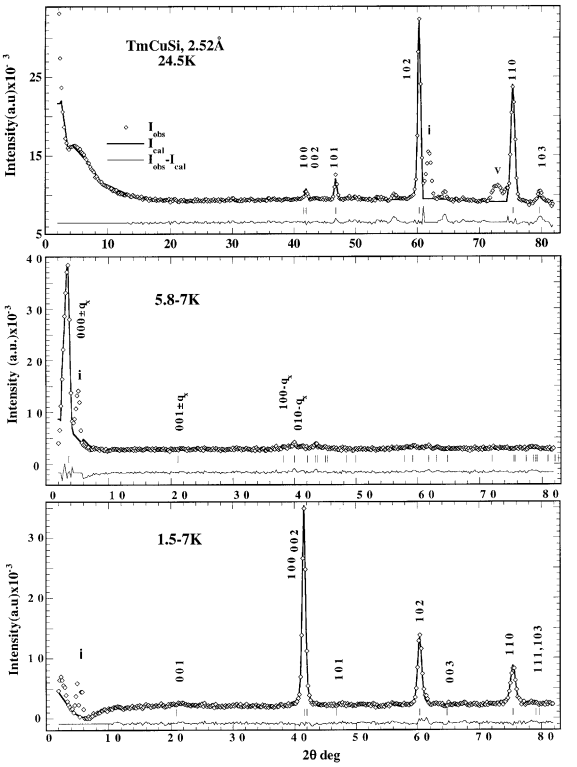

Fig. 2. Observed and calculated (D1B) neutron patterns of TmCuSi, in the paramagnetic state at 24.5 K (top part). The excluded region at 71(•) is from a V line of the cryostat. Representative difference diagrams of the magnetically ordered state are given at: 5.8–7 K (middle part) and 1.5–7 K (bottom part). These patterns comprise exclusively magnetic reflections in order to avoid magnetic impurity contributions.

D20 (high flux) at the facilities of the ILL in Grenoble with $\lambda = 2.52$ and 2.4198 Å, respectively. The use of the two instruments in the present case is complementary. The D1B high flux instrument provides information in the low 2θ angle range, which is crucial in the study of incommensurate magnetic structures common in rare earth compounds, as the detection of the wave vector within the first Brillouin zone is the most important step in the analysis of powder diffraction data. The step increment of the scattering angle 2θ and the 2θ range was 0.2° and 1.8–81.8° for the D1B instrument, and 0.1° and 7–154.2° for the D20 instrument. The data collection with the D20 instrument became indispensable in the study of the magnetic phase diagram of TmCuSn as the HT

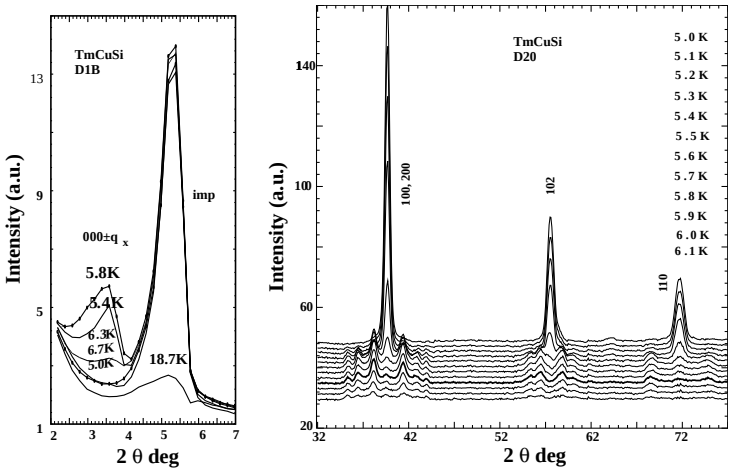

Fig. 3. Left part, D1B data: low-angle antiferromagnetic peaks for various temperatures in TmCuSi above and below T_N and T_C. The intensity of the TmCuSi zero point satellite $(0\,0\,0)\pm\mathbf{q}_1$ at $2\theta = 3.5(^\circ)$ changes drastically in the temperature range 5–6.7 K while the impurity peak at 5.3° remains almost unchanged and disappears above 19 K. Right part D20 data: Thermogram of the temperature range 5.0–6.1 K showing the crossover from antiferromagnetism to ferromagnetism at 5.8 K (thick line).

range where the magnetic intensities are very weak was found to be of particular interest. The step increment in temperature was 0.3–0.5 K in D1B while for the D20 instrument the step was 0.1 K. The data were corrected for absorption and evaluated by the FullProf Program [10]. Results are summarised in Figs. 2–4,6,7.

3. Results and discussion

3.1. Crystal structure

The 24.5 K neutron D1B data obtained in the paramagnetic state were refined using the reported model of the Ni_2In structure shown in Fig. 1 ($P6_3/mmc$ space group). Results are summarised in Table 1 and Fig. 2 (top part). Two impurity lines were left out of consideration by excluding the corresponding regions: one at $2\theta = 71^\circ$, due to the V line of the cryostat and the other at 62°, being unidentified.

3.2. LT magnetic ordering

The 1.5 K D1B neutron data display a few magnetic reflections superimposed on the nuclear

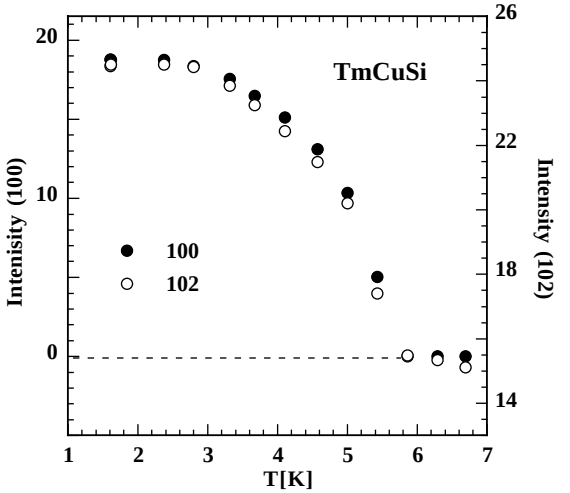

Fig. 4. Temperature dependence of the strongest ferromagnetic intensities of (1 0 0) and (1 0 2) reflections.

reflections while a strong peak at $2\theta = 5.2^\circ$ and two further weak peaks (at 2θ, 15.2° and 35°) cannot be indexed by the Ni_2In type of structure or any simple multiple cell of it. These were left out of consideration in the refinements as they display a different thermal behaviour (Fig. 3 left part) and disappear at a temperature (19.2 K) much higher than that expected for ordering of TmCuSi. The

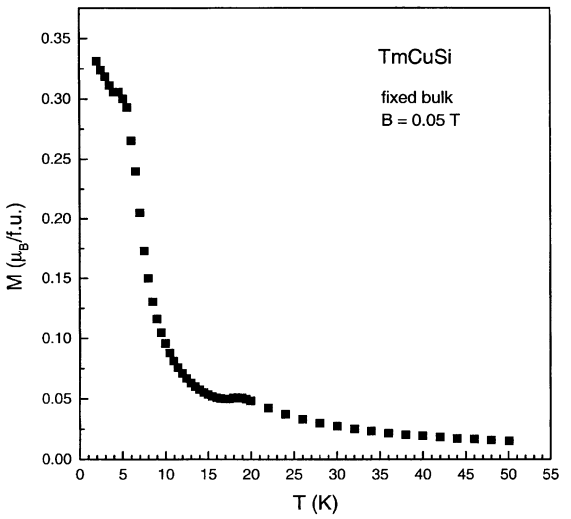

Fig. 5. Temperature dependence of the magnetisation measured on a fixed bulk piece of polycrystalline TmCuSi in a field of 0.05 T. The shallow maximum at about 19 K corresponds to antiferromagnetic ordering of the impurity phase.

simplest assumption was that they pertain to the unidentified impurity phase and for this reason the refinements were carried out on the basis of the difference diagrams by subtracting the 7 K data (Fig. 2). A small part of the strong foreign magnetic impurity is still visible at lower temperatures at $2\theta = 5.2^\circ$ in Fig. 2 (bottom part).

The refinement of the difference diagrams confirmed the ferromagnetic ordering of the Tm magnetic moments and the reduced ordered moment value at 1.5 K of $6.2(1)\,\mu_B$/Tm atom relatively to the Tm^{3+} free ion moment value of $g\mu_B J = 7\,\mu_B$ in good agreement with the results given in Ref. [9]. However, there are some differences in the model concerning the moment direction that was found to deviate by $\Phi_c = 18(1)^\circ$ from the *c*-axis and the ordering temperature. The temperature dependence of the ferromagnetic peaks (1 0 0) and (1 0 2) shown in Fig. 4 makes it clear that the ferromagnetic ordering is stable below 5.8 K and not below $T_C = 9$ K as found in Ref. [9]. The former temperature corresponds closely to a discontinuity in the temperature dependence of the magnetization shown in Fig. 5 and will be called T_C in the following.

The middle part of Fig. 2 shows that the diffraction behaviour in the 5.8–7 K data is

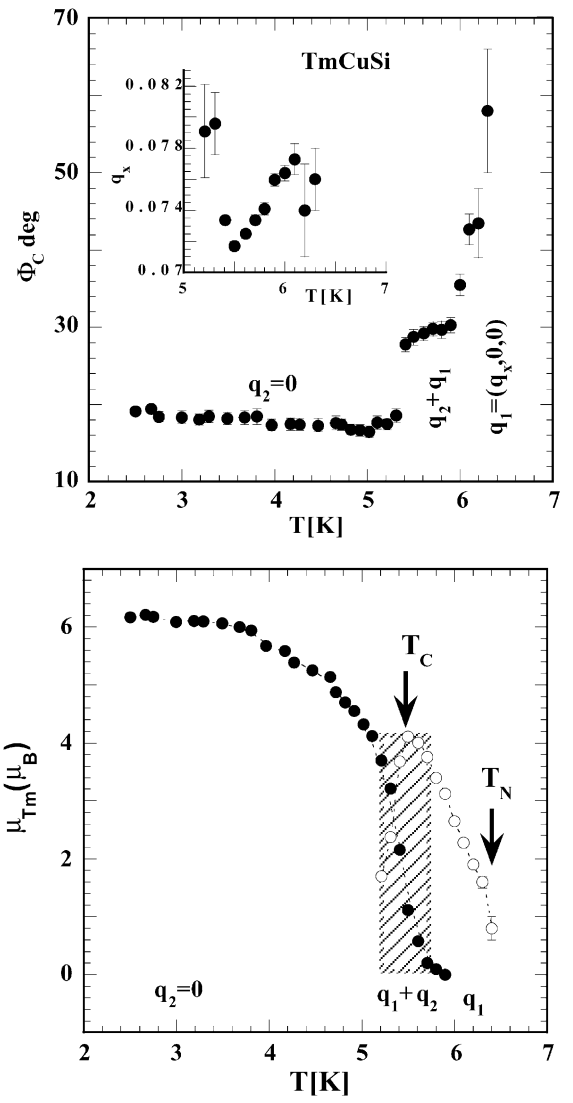

Fig. 6. Thermal variation of the Tm magnetic moment angle with the *c*-axis (top part) showing a discontinuity in the transition range from the ferromagnetic to antiferromagnetic state. The inset shows the temperature dependence of the wave vector length over the transition range. Also shown is the thermal variation of the Tm ordered moment and/or amplitude value tracing the magnetic phase diagram (bottom part).

completely different from that of the ferromagnetic ordering. In fact the strong satellite close to the origin demonstrates the transition to an antiferromagnetic state. The spurious weak peaks occur on both sides of the nuclear reflections

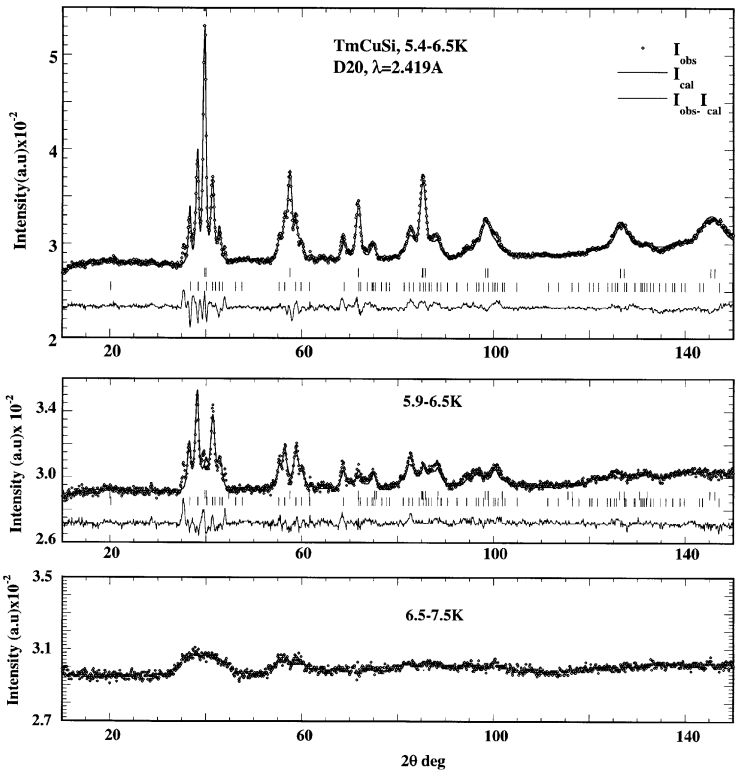

Fig. 7. Observed and calculated D20 neutron difference diagrams of TmCuSi, for two temperatures in the *HT* region above the first-order transition (top and middle part) and at $T_N = 6.5\,K$ where short-range order effects are present (bottom part).

Table 1
Crystal and magnetic structure refinement results of TmCuSi from D1B neutron data

Parameter	24.5 K	1.5–7 K
a (Å)	4.141(4)	4.141
c (Å)	7.104(11)	7.104
μ_z, (μ_B),		6.2(1)
Φ_C (°)		18(1)
R_B, R_m (%)	4.7, —	—, 10
R_{wp}, R_{exp} (%)	8, 5	7.7, 5.6

Space group $P6_3/mmc$ with Tm at 2*a*: (0, 0, 0); Cu at 2*c*: (1/3, 2/3, 1/4) and Si at 2*d*: (1/3, 2/3, 3/4). $R_B, R_{m1}, R_{wp}, R_{exp}$ are the residuals for the integrated Brag and magnetic, the weighted profile and the experimental intensities. The overall temperature factor *B*(of) was fixed to zero.

(1 0 0/0 0 2) and at higher angles become clearly visible in the D20 data. This peak topology suggests a wave vector along the hexagonal *a*-axis $\mathbf{q}_1 = (q_x, 0, 0)$ similar to ErCuSi [8]. A systematic analysis of the D20 data has shown that the angle Φ_c the Tm moments make with the *c*-axis remains unchanged in the 1.5–5.4 K temperature region (see Fig. 6 top part) but increases discontinuously at about 5.4 K (on heating) where the magnetic structure undergoes a first-order transition to an incommensurate phase as will be discussed below.

3.3. The amplitude modulated magnetic structure $\mathbf{q}_1 = (q_x, 0, 0)$

Fig. 3 presents parts of reciprocal space in the temperature range 5.0–6.7 K, which are relevant in the description of the crossover from ferromagnetic to antiferromagetic ordering. The left part of the figure displays the low angle D1B data and is restricted to the thermal evolution of the zero point satellite at $2\theta = 3.7°$, which is the strongest magnetic peak. The magnetic intensity becomes discernable from the background only above 5 K

(on heating) and continues to increase till about 5.8 K where it starts to decrease and finally disappears at $T_N = 6.5$ K, while the impurity peak at $2\theta = 5.3^\circ$ is still detectable in the 18.7 K pattern included in the figure.

The high flux of the D20 instrument and the 0.1 K step in temperature used in the acquisition on heating of the difference thermogram (by subtracting the 6.5 K nuclear intensities) shown in Fig. 3 (right part), allow a better insight in this seldom phenomenon. At the highest shown temperature of 6.1 K (first curve from below) only $\mathbf{q}_1$ satellites are visible on both sides of the (1 0 0, 2 0 0) reflection position. Their intensity at T_C (fat curve) is much stronger if compared with the D1B data of Fig. 2 (middle part). Weak ferromagnetic reflections ($\mathbf{q}_2 = 0$) become detectable at 5.8 K (fat curve) and their intensity increases at the cost of the $\mathbf{q}_1$ satellites at lower temperatures. The faster increase of the ferromagnetic intensities is just below 5.4 K. The intensity of the $\mathbf{q}_1$ phase disappears at about 5 K.

Refinements of several data sets collected with both instruments over the entire ordered regime but in particular those of the D20 data allowed us to derive a detailed magnetic phase diagram. The moment angle with the *c*-axis was constrained to the same value for the coexistence region of the two phases as the moment direction is fixed by the crystal field and does not depend on the sign of the exchange interaction. The refinements of the incommensurate phase were carried out using a sine wave model for the Tm moments as no higher harmonics were observed in the neutron pattern. The residuals of the calculations were around 10–14% for R_{wp} (weighted profile) and 3–8% for the magnetic R_m of the two phases in the LT range.

Fig. 7 displays the refined patterns below and above T_C. The difference diagram 6.5–7.5 K shows the presence of short-range order effect at the same positions where the magnetic satellites appear just below T_N. For the 5.9 K data comprising exclusively the $\mathbf{q}_1$ phase the refined parameters are: $q_x = 0.0760(5)$, the refined amplitude of the wave is $\mu_0 = 3.12(1)\,\mu_B$/Tm atom and $\Phi_c = 30(1)^\circ$. The weighted profile R_{wp} and the magnetic residuals R_m were 24% and 8.6% and $\chi^2 = 1.7$. At 5.4 K the two phases are present almost in equal amounts: for the $\mathbf{q}_2 = 0$ phase $\mu_F = 2.12(1)\,\mu_B$/Tm, $\Phi_c = 28(1)^\circ$ for the $\mathbf{q}_1$ phase $q_x = 0.0734(2)$, and $\mu_0 = 3.68(2)\,\mu_B$/Tm atom. $R_{wp} = 14\%$, $R_{m1} = 3.7\%$ and $R_{m2} = 8\%$ and $\chi^2 = 4.5$. A few additional magnetic peaks at 2θ 38°, 40°, 42° in the difference diagrams at 5.4–6.5 and 5.9–6.5 K (Fig. 7) suggest the presence of small amounts of a second magnetic phase with a larger wave vector value. However, their weak intensity did not allow an accurate refinement. The moment value μ_{nj} of the *j*th atom in the *n*th cell in a sine wave modulated structure may be derived from the moment value (Fourier coefficients) in the zeroth cell:

$$\begin{aligned}\mu_{nj} &= \sum_{\{\mathbf{q}\}} \mathbf{S}_{\mathbf{q}_j} \exp\{-2\pi i \mathbf{q}\cdot\mathbf{R}_n\} \\ &= \mu_0 \cos\cos(2\pi \mathbf{q}.\mathbf{R}_n + \phi) \\ &= \mu_{0,j}\mathbf{z}\cos(2\pi\mathbf{q}\cdot\mathbf{R}_n + \phi), \end{aligned} \quad (1)$$

where $\mathbf{R}_{nj} = \mathbf{r}_j + \mathbf{R}_n$ with $\mathbf{R}_n = n_1\mathbf{a}+n_2\mathbf{b}+n_3\mathbf{c}$, in the *n*th cell (*n* is integer and $j = 1$), $\mathbf{z}$ is a unit vector in the direction of the varying moment component, μ_{0i} the amplitude of the sinusoidal variation and ϕ_j, a phase factor of the *j*th atom relative to the origin of the wave usually taken at atom (1). Symmetry analysis has shown that the Tm atoms at *2a* belong to the same orbit and have therefore the same moment value. As the phase of Tm at $(0,0,1/2)$ was found to be zero, the structure can be fully described only for the Tm atom at $(0,0,0)$ and by using expression (1) for deriving the moment value for *n* cells.

4. Conclusion

The refinement of neutron data at various temperatures of the TmCuSi compound confirms the hexagonal $InNi_2$ type of structure proposed by several investigators as well as the low-temperature ferromagnetic ordering described in Ref. [9]. However, the ferromagnetic ordering occurs only below $T_C = 5.8$ K and is preceded by a narrow high-temperature (HT) antiferromagnetic region extending from 5.0 to $T_N = 6.5(1)$ K. This region is associated with an incommensurate phase with the wave vector $\mathbf{q}_1 = (q_x, 0, 0)$ having a temperature-dependent length. The Tm moments deviate from

the c-direction by a constant angle of 18° in the LT range but this angle increases drastically above the antiferromagnetic transition. This easy moment direction deviates from that proposed for a low-symmetry R site with point symmetry 3 m (D_{3d}), suggesting a moment direction parallel to c for both the Er and Tm atoms on the basis of a point-charge crystalline field calculation with a predominant second-order term [11]. The difference in moment direction observed for ErCuSi (where the magnetic moments are confined to the c-axis) and TmCuSi (where they deviate from the c-direction by a constant angle of 18° indicates that crystal field terms of order higher than two are required for describing the anisotropy in the RCuSi compounds.

The crossover from antiferromagnetism to ferromagnetism occurs via a first-order transition that could be closely followed using the D20 high flux data with a very small step in temperature. The presently available results are summarised in a magnetic phase diagram of TmCuSi displayed in Fig. 6 (bottom part). It comprises three regions: a (HT) region $T_C = 5.8\,K \leqslant T < T_N$ characterised by the presence of a single wave vector $\mathbf{q_1} = (q_x, 0, 0)$ pertaining to an amplitude modulated phase, a (LT) ferromagnetic region $1.5 \leqslant T < 5\,K$ with $\mathbf{q}_2 = 0$ and a narrow intermediate region $5.4 \pm 0.4\,K$ where the magnetic ordering is associated with the two wave vectors $\mathbf{q_1} = (q_x, 0, 0)$ and $\mathbf{q}_2 = 0$. Most probably the latter two structures coexist in the form of different domains. However, the existence of an intermediate type of structure cannot be ruled out on the basis of the present diffraction data.

The occurrence of incommensurate magnetic phases is a generally observed phenomenon in collinear magnetic structures of rare earth metals and compounds, where the crystal field ground state is magnetic [1,12]. The magnetocrystalline anisotropy imposes the moment directions while the formation of incommensurate structures is a consequence of the long-range oscillatory character of the RKKY exchange interaction mediated via the conduction electrons. As a rule, sine wave structures square up at lower temperatures for thermodynamic reasons. A sequence of transitions from a (antiferromagnetic) spiral to a conical or more complex structure has been frequently observed in the hexagonal rare earth metals and their binary or ternary compounds with 3d metals, i.e. in Er and Ho [13] and in $TbMn_6Ge_6$ [14]. In the latter compound one observes a reentrant ferrimagnetism arising from the interplay of competing ordering mechanisms of the two magnetic systems with different anisotropies leading to a sequence of transitions from a HT $x-y$ ferrimagnetic phase to an IT flat spiral and a LT cone. In this case the wave vector length was decreasing continuously with increasing temperature and reached zero at the HT ferrimagnetic transition. The crossover from an antiferromagnetic sine wave to antiphase domain $(+\,+\,+\,+\,-)$ uncompensated magnetic structure with a resultant ferromagnetic component has been observed in hexagonal Tm. This transition was evidenced by the presence of higher harmonics, one of which coincided with the nuclear reflections [13]. A first-order transition from an incommensurate phase to a ferromagnetic one has been found in the tetragonal $NdRu_2Si_2$ and $NdRu_2Ge_2$ compounds [15–17]. The $NdRu_2Si_2$ phase with the wave vector $\mathbf{q} = (0.13, 0.13, 0)$ undergoes a squaring-up transition manifested by the presence of higher harmonics to prior to the ferromagnetic transition. The $NdRu_2Ge_2$ phase [17] is involving two wave vectors $q = (0.12, 0.12, 0)$ and $q = (0.19, 0.05, 0.125)$ with a temperature-dependent length. Some subtle sample-dependent differences [16] exist in the transition mechanism between polycrystalline and single crystal samples of $NdRu_2Si_2$. Chevalier et al. [15] report a statistical distribution between Ru and Si sites for exclusively the RRu_2Si_2 (R = Nd,Tb) compounds in powder samples. In spite of some differences between the two phases, the stable low-temperature phase is the ferromagnetic one for both compounds. In the case of ErCuSi, the onset of the squaring-up transition was manifested by the appearance of $3\mathbf{q}$ higher harmonics ($q_x = 0.08333$) [8]. The behaviour of TmCuSi is, however, different from the behaviour of all the compounds discussed above. The wave vector length found in TmCuSi is smaller than that of the ErCuSi compound and decreases with decreasing temperature from $q_x = 0.078$ to 0.071 in the HT range and jumps to zero at T_C. Furthermore,

no higher harmonics become visible as in the ErCuSi compound. It is possible that due to the smaller value of the wave vector length $q_x = 0.071(1)$ at 5.5 K the wave vector jumps faster to zero in parts of the sample which might have a slight magnetic disorder possibly originating from a small degree of Cu/Si site disorder. The magnetically disordered regions, having a non-zero net magnetization, in turn might produce a magnetic field along the moment direction of the incommensurate phase with the interesting end effect of crossover from antiferromagnetism to ferromagnetism. Alternatively the change in magnetic order could be attributed to other factors that influence the competition between the ferro- and antiferromagnetic (bilinear) interactions such as quadrupolar pair interactions, which have been reported to be large in rare-earth intermetallic compounds [18], especially those of Pr^{3+} and Tm^{3+}. The variety of different low-temperature behaviours of incommensurate phases demonstrates the delicate balance between the competing factors governing the magnetic order.

References

[1] A. Szytula, in: K.H.J. Buschow (Ed.), Handbook of Magnetic Materials, Vol. 6, Elsevier Science, Amsterdam, 1991, p. 85.
[2] W. Rieger, E. Parthé, Mh. Chem. 100 (1969) 439.
[3] A. Iandelli, J. Less-Common Met. 90 (1983) 121.
[4] A. Mugnoli, A. Albinati, A.W. Hewat, J. Less Common Met. 97 (1984) L1.
[5] H. Oesterreicher, Phys. Stat. Sol. A 34 (1976) 723.
[6] H. Kido, T. Hoshikawa, M. Shimada, M. Koizumi, Phys. Stat. Sol. A 77 (1983) K121.
[7] W. Bazela, A. Szytula, J. Leciejewicz, Solid State Commun. 56 (12) (1985) 1043.
[8] P. Schobinger-Papamantellos, K.H.J. Buschow, N.P. Duong, C. Ritter, J. Magn. Magn. Mater. 223 (2001) 203.
[9] Y. Allain, F. Bourée-Vigneron, A. Oles, A. Szytula, J. Magn. Magn. Mater. 75 (1988) 303.
[10] Rodríguez-Carvajal, J. Physica B 192 (1993) 55. The manual of FullProf can be obtained from a Web browser at http://www-llb.cea.fr/fullweb/powder.htm.
[11] J. Rossat-Mignod, J. Yakinthos, Phys. Stat. Sol. 47 (1971) 239.
[12] D. Gignoux, D. Schmitt, Phys. Rev. B 48 (17) (1993) 12682.
[13] W.C. Koehler, J. Appl. Phys. 36 (1965) 1078.
[14] P. Schobinger-Papamantellos, J. Rodriguez-Carvajal, G. André, K.H.J. Buschow, J. Magn. Magn. Mater. 150 (1995) 311.
[15] B. Chevalier, J. Etourneau, P. Hagenmuller, S. Quezel, Rossat-Mignod, J. Less-Common Met. 111 (1985) 161.
[16] D. Gignoux,D. Schmitt, in: K.H.J Buschow (Ed.), Handbook of Magnetic Materials, Vol. 10, Elsevier, Amsterdam, 1997, p. 239.
[17] A. Szytula, A. Oles', M. Perrin, M. S'laski, W. Kwok, Z. Sungaila, B.D. Dunlap, J. Magn. Magn. Mater. 69 (1987) 305.
[18] P. Levy, P. Morin, D. Schmitt, Phys. Rev. Lett. 42 (1979) 1417.